The Interplanetary Causes of Magnetic Storms, Substorms and Geomagnetic Quiet

B.T. Tsurutani
Jet Propulsion Laboratory, California Institute of Technology

Key words: Space weather, substorms, magnetic storms, auroras

Abstract The current knowledge of the interplanetary and solar causes of superstorms ($D_{ST} \leq -350$ nT), major magnetic storms ($D_{ST} \leq -100$ nT), recurring substorms and HILDCAAs will be summarized. The causes of geomagnetic quiet during both solar maximum and solar minimum will also be reviewed. The discussion will start with geomagnetic activity during the solar maximum portion of the solar cycle and then that of the declining phase. A newly identified type of aurora, that caused by interplanetary shocks, will be discussed. Such auroras may occur at other planets as well.

1. INTRODUCTION

I will start this lecture with a few illustrative questions to help orient the beginner to the field of space physics. The questions are meant to be provocative ones, in that they address some common misconceptions held by the uninitiated. The answers will be given without explanations for the time being. Explanations to the answers will all be contained within the text of this chapter.

1. Do Coronal Mass Ejections (CMEs) from the sun (which hit the Earth's magnetosphere) cause geomagnetic storms at Earth? Answer: Sometimes.

2. If the Interplanetary Coronal Mass Ejections (ICMEs) have southwardly directed magnetic fields, *then* will this be sufficient to cause magnetic storms? Answer: No, not necessarily.

3. (Corollary to 2): Since the ICME fields will be equally northwardly and southwardly directed, then shouldn't at least half of all ICMEs (which impinge upon the Earth) cause magnetic storms? Answer: No.

4. Since the answers to the previous three questions were "No" or "Sometimes", then why are CMEs/ICMEs important at all? Answer: For *fast* ICMEs, the solar ejecta material and their upstream sheaths (behind the shocks) contain *intense* magnetic fields giving them a *statistically higher probability* of the right conditions to generate magnetic storms.

5. What are the necessary interplanetary conditions for the generation of large magnetic storms? Answer: Intense hours-long duration, southwardly directed magnetic fields ($B_Z < -10$ nT, $\tau > 3$ hrs).

6. What are the solar and interplanetary causes of the very biggest magnetic storms (superstorms)? Answer: At this time we are not sure. But I will make some speculations based on what we presently know.

References: 1. Tsurutani et al., 1988a and references therein. 4. Tsurutani et al. (1988b). 5. See Gonzalez and Tsurutani (1987); Gonzalez et al. (1994), Kamide et al. (1998a,b). 6. Tsurutani et al. (1992, 1999).

2. MAGNETIC STORM HISTORY

Mankind has certainly detected the effects of magnetic storms before written history took place. Red auroras are easily observable at midlatitudes during intense storms. Using lodestones, strong terrestrial magnetic deflections would have been obvious when the observer was under the auroral electrojet. One of the first published paper on magnetic storms was written by Baron Alexander von Humboldt* in *Annales der Physik* (1808). In the paper, von Humboldt described the results of an experiment performed from his home in Berlin, Germany, on 21 December 1806. Every half hour he and a colleague used a microscope to observe magnetic declinations of small magnetic needles. This was done from midnight to early morning. Von Humboldt noted that there were auroras overhead. He also noticed that when the northern lights disappeared at dawn, the magnetic needle deflections died out. He called this geomagnetic activity interval a

"Magnetisches Ungewitter", or a "magnetic storm". This is the origin of the name of the phenomenon. (Von Humboldt was the first to study the geography, geology, and climatology of South America, leading to modern geophysics. He also founded the "Magnetische Verein" whose members included Gauss and Weber.)

These magnetic variations that von Humboldt saw and reported on are associated with the auroral electrojet which typically flows at a ~100 km altitude and at ~65° magnetic latitude in the local midnight sector. The currents have nominal intensities of $\sim 10^6$ Amperes during substorms. During intense geomagnetic activity (magnetic storms), the electrojet moves to lower latitudes and can be even more intense. The auroral electrojet during extreme events may cause fields at the Earth's surface to be as large as several thousand nanotesla (nT), or Earth magnetic field deviations of up to ~10%.

What is standardly used as a signature of a magnetic storm is an index formed from the output of four or more ground-based magnetometers located at or near the magnetic equator. This average deflection (taking out diurnal variations due to Sun-lit ionospheric current systems) is called the D_{ST} index, first proposed and constructed by Sydney Chapman. This index was adapted by a working group of the 1975 Grenoble IUGG.

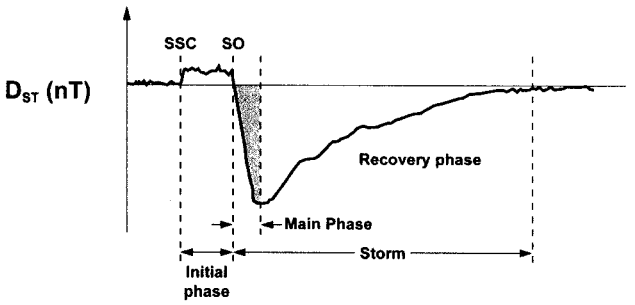

Figure 1. A profile of an idealized magnetic storm during solar maximum, as measured by ground based near-equatorial magnetometers (D_{ST} index).

The magnetic field magnitude profile of a magnetic storm occurring near solar maximum is shown in Figure 1. The storm has three phases: an "initial phase" where the magnetic field increases anywhere from +10 to +50 nT, a "main phase" where the field magnitude decreases by 100 (or more) nT, and a recovery phase where the field gradually recovers to the ambient value. The initial phase typically starts suddenly (<5 min duration) and lasts an indeterminate amount of time. It may or may not be followed by a storm

main phase (these first two phases, the initial and main phases, will be shown to be caused by different physical phenomena). The main phase can be as short as an hour or as long as a day. The recovery phase typically lasts 7 to 10 hours (Chapman and Bartels, 1940).

The sudden sharp jump in the Earth's field at the onset of the initial phase (Storm Sudden Commencement or SSC) is caused by the abrupt increase in the solar wind ram pressure at interplanetary shock (Araki et al., 1988). The plasma density (and magnetic field) across the shock increases by a value which is approximately the shock Mach number (Kennel et al., 1985). For typical interplanetary shocks, the Mach number ranges from 1 to about 3 (Tsurutani and Lin, 1985). Although the shock thickness is only ~ seconds in width, after the shock hits the magnetosphere, the compressional wave travels at the magnetosonic wave speed from multiple points of the outer magnetosphere. Thus, the SSC temporal width measured at the surface of the Earth is much broader, typically ~mins wide (Araki et al., 1977).

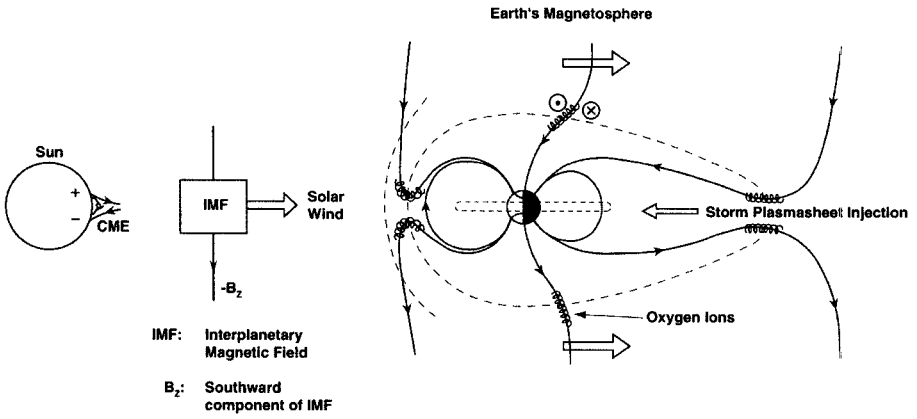

Figure 2. A schematic of magnetic reconnection between interplanetary magnetic fields and the Earth's field. Note that, in this scenario, plasma injection into the magnetosphere occurs near midnight, explaining the local time dependence of auroras.

The storm main phase is caused by magnetic interconnection between interplanetary magnetic fields and the Earth's field (Dungey, 1961; Gonzalez and Mozer, 1974). This process is most efficient when the interplanetary fields are directly opposite to that of the Earth's field at the magnetopause. or a southward direction. This is shown in Figure 2, an adaptation of a schematic from Dungey (1961). The interconnected field lines are dragged back by the solar wind plasma and reconnect in the nightside magnetotail. When the fields are reconnected once more, the release of magnetic tension causes the entrained plasma to be sling-shotted from the tail towards the

Earth to the near midnight sector of the magnetosphere. The energetic plasma on the closed magnetic field lines exhibits three adiabatic motions (Alfvén and Fälthammer, 1963; Northrup, 1961): 1) a particle gyromotion about the magnetic field, 2) a bounce motion up and down the field within the "magnetic bottle", and 3) azimuthal motions around the dipole field. These three particle motions are illustrated in Figure 3. For singly charged particles, electrons drift from midnight towards dawn due to the presence of magnetic curvature and field gradients, and the ions drift from midnight toward dusk due to the same causes. Because the oppositely charged particles drift in opposite directions, these drifts form a current. This ring of current decreases the Earth's magnetic field (a diamagnetic current), and is called the "ring-current".

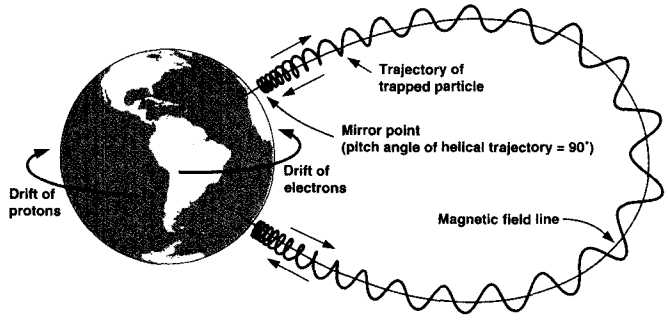

Figure 3. Charged particle motions in the magnetosphere. The three adiabatic motions are illustrated.

The near-equatorial field decrease that occurs during the storm main phase is caused by the formation and injection of this ring-current deep into the magnetosphere. Dessler and Parker (1959) and Sckopke (1966) have shown that the magnitude of the field decrease is linearly related to the total particle kinetic energy of the ring-current. Other current systems can certainly contribute significantly to D_{ST}, but it is currently being debated as to how much an effect this is (Campbell 1999; Kamide et al., 1999; Singer et al. 2000).

There are two regions associated with fast ICMEs where the magnetic fields might be sufficiently intense to cause a magnetic storm main phase: a magnetic cloud region within the ICME (Klein and Burlaga, 1982) and the interplanetary sheath (Tsurutani et al., 1988b; Tsurutani and Gonzalez, 1997), located upstream (antisunward) of the ICME and behind the shock.

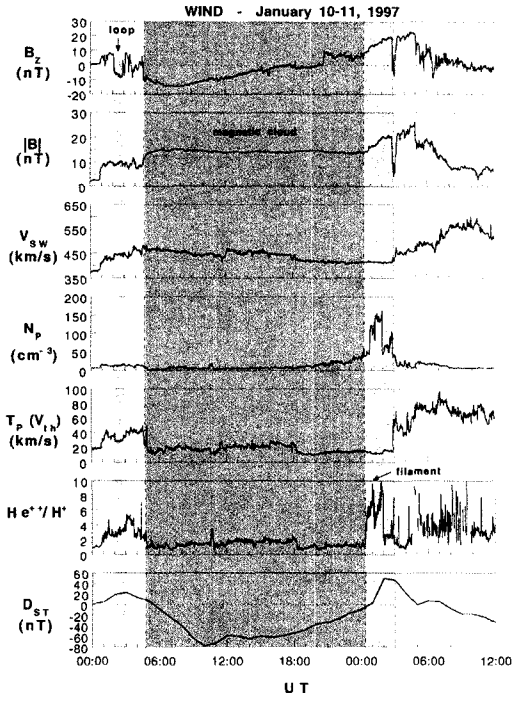

Figure 4. The January 10, 1997 example of a magnetic cloud event causing the main phase of a magnetic storm. Magnetic clouds are parts of ICMEs/driver gases.

An example of a magnetic cloud event causing a magnetic storm is shown in Figure 4. It is the well-studied January 10, 1997 event (Fox et al., 1998). D_{ST} is noted to decrease coincident with the intense, smoothly varying southward magnetic field of the cloud, supporting the hypothesis that the solar wind energy transfer mechanism is indeed magnetic reconnection.

The storm recovery phase is associated with the loss of the ring-current particles from the magnetosphere. Physical processes for the loss are: convection of plasma out the dayside magnetopause, charge-exchange with atmospheric neutral particles, Coulomb collisions, and wave-particle resonant interactions. See Kozyra et al. (1997) for a general discussion of wave-particle loss processes. Further, it has been noted that the physics of particle losses is extremely complex. The "decay time" depends on the particle energy, species, pitch angle and location, thus there is an infinite number of τ values, not simply a single "7 to 10 hour" value as stated earlier. Daglis (this book) has pointed out that during the peak phase of the storm, oxygen ions dominate the ring-current energy densities. These particles are lost most rapidly with time scales of ~1-2 hours.

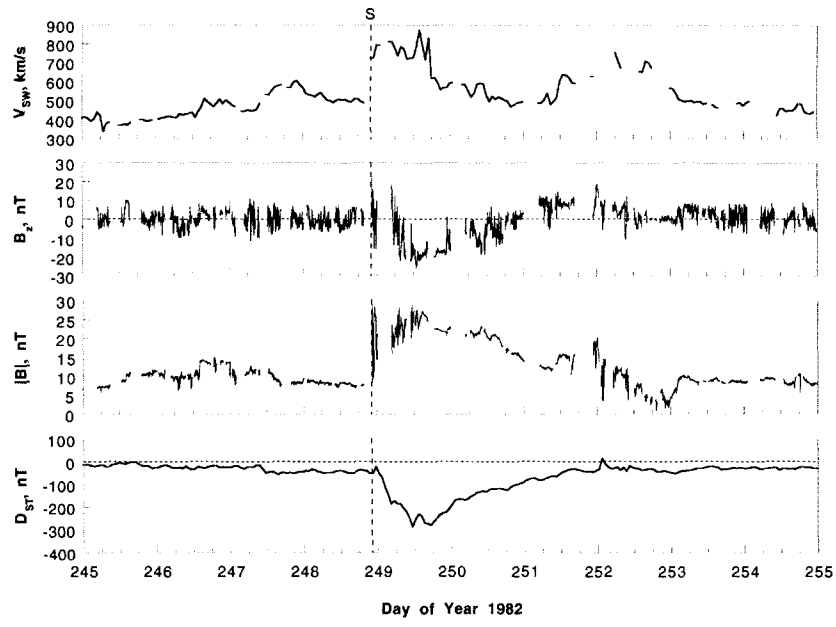

Figure 5. The September 1982 interplanetary shock event. Solar wind velocity, and magnetic field z-component and magnitude measured by ISEE-3 are shown, along with D_{ST} data. The southward magnetic fields creating the storms are sheath fields.

An example of an interplanetary sheath B_S event leading to a major magnetic storm is shown in Figure 5. The shock is indicated by the dashed vertical line. There is intense interplanetary B_S just behind the interplanetary shock. The former causes the storm main phase. The IMF B_S increase behind the shock is most probably due to shock compression of the upstream slow stream IMF B_S.

3. AURORAS

What causes auroras during magnetic storms? When the plasma is sling-shotted into the magnetosphere, both the electrons and ions are "compressed" such that their perpendicular temperatures become higher than their parallel temperatures. Such anisotropies lead to instabilities like the loss-cone instability (Kennel and Petschek, 1966). One consequence of such instabilities is the growth of electromagnetic plasma waves called chorus, shown in Figure 6 (Tsurutani and Smith, 1974). The waves through cyclotron resonant interactions pitch-angle scatter the particles (Tsurutani and Lakhina, 1997), leading to their loss to the upper

atmosphere/ionosphere. The precipitating particles lose their kinetic energy through collisional excitation processes. Resultant excited ionospheric atoms and molecules decay to their ground state giving off characteristic auroral light.

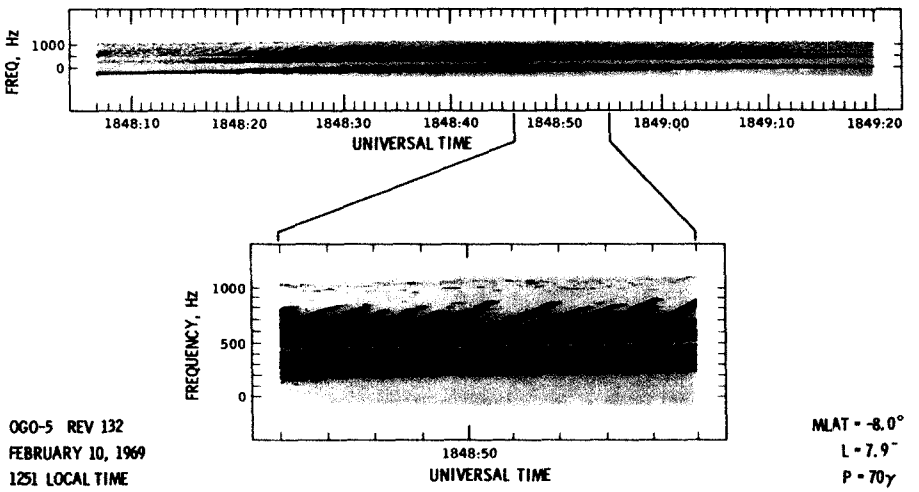

Figure 6. Magnetospheric electromagnetic whistler mode chorus emissions. These emissions are produced by the electron loss-cone instability.

Strong cross-magnetospheric convection electric fields with concomitant field-aligned potentials are also a consequence of magnetic reconnection and strong magnetic field distortions (Haerendel, 1994). Parallel electric fields above the ionosphere lead to the downward acceleration of electrons to energies of 1-10 keV and from their loss, to the formation of auroral arcs. A schematic taken from Elphic et al. (1998) showing upward and downward current systems, is given in Figure 7. An image of a long auroral arc taken from the Space Shuttle is given in Figure 8. The accelerated electrons come down magnetic field lines and lose their energy by collisional excitation. A red auroral fringe at the highest altitudes is due to a 6300 Å line from the metastable decay of atomic oxygen. The decay is present above 200 km altitude where the collisional de-excitation time is longer than the ~200s for the natural (metastable) decay. The blue-green oxygen light at lower altitudes is a mixture of oxygen 5577 Å and nitrogen 3914 Å lines.

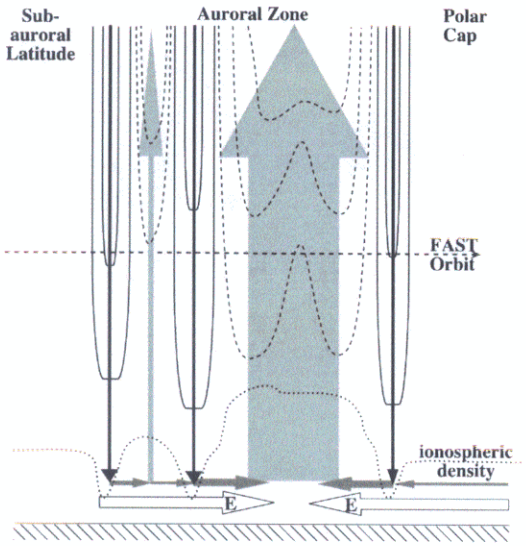

Figure 7. A schematic of field-aligned currents and the acceleration of electrons which form auroral arcs.

During magnetic storms, pure red (6300 Å) auroras are also produced at lower than normal latitudes. The exact physical mechanism is unknown at this time (see other articles of this book). These red auroras occur during the storm recovery phase. Figure 9 is an example of an event that was seen at the Jet Propulsion Laboratory's Table Mountain Observatory (near Los Angeles, California) during an intense magnetic storm on April 12, 1981 (courtesy of J. Young).

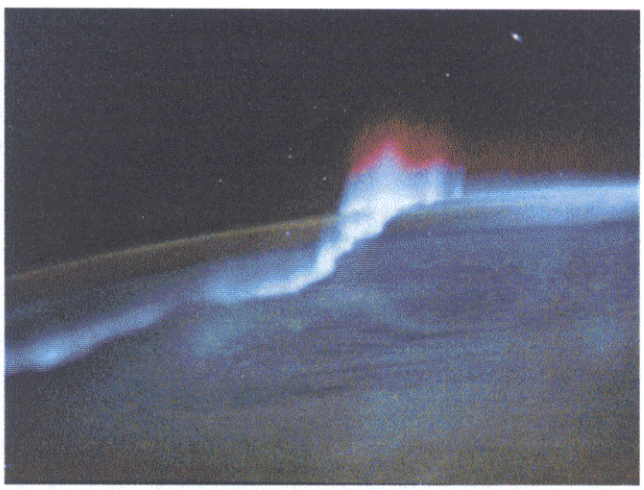

Figure 8. An auroral arc photographed from the Space Shuttle.

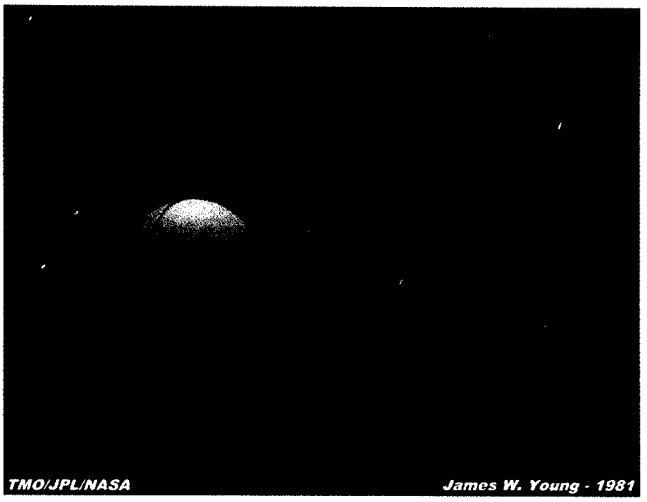

Figure 9. A photograph of a red aurora taken during the April 1981 magnetic storm. The photograph was taken near Los Angeles, California.

4. SOLAR MAXIMUM

4.1 Super-intense Storms

What causes super-intense storm events that can produce ground power outages, major satellite damage and satellite losses? There are a number of possibilities, but unfortunately we do not know for certain. We have data on too few events to really understand all of the causes at this time. However, we can make some reasonable speculations.

4.1.1 High Velocity CMEs

Single, violent CME events could lead to superintense storms. Gonzalez et al. (1998) have shown that there is a statistical relationship between the peak magnetic field magnitude within an ICME at 1 AU and its velocity (Fig. 10). This empirical relationship is most likely due to the CME release

and acceleration mechanism occurring near the Sun. However, computer simulations need to be performed to verify this speculation.

Not shown in Figure 10 are the particularly high fields and velocities of the August 1972 ICME event (see discussion in Tsurutani et al., 1992). This general V_{SW} - |B| relationship holds for this extreme event as well.

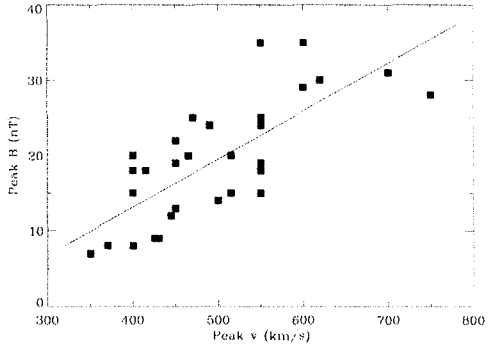

Figure 10. An empirical relationship between the interplanetary magnetic field strength and the speed of magnetic clouds.

4.1.2 Multiple ICMEs (Multiple Flaring at the Sun)

Shock compression of high intensity magnetic fields is a process which, under the right conditions, can lead to even higher magnetic field strengths. Figure 11, taken from Lepping et al. (1997) shows one such "double" event. The compression at point C is most likely shock compression within a magnetic cloud. However, we note that the plasma beta (β equals plasma thermal pressure divided by magnetic pressure) within clouds is generally lower than the present case (Tsurutani and Gonzalez 1997; Farrugia et al., 1997), so events similar to this one should be rare (note that the compression is present only where the β is somewhat high). For low beta plasmas, the magnetosonic wave speeds can be comparable or even higher than the solar wind speeds, so shock waves in magnetic clouds will become evanescent. There should be little or no magnetic compression for these cases.

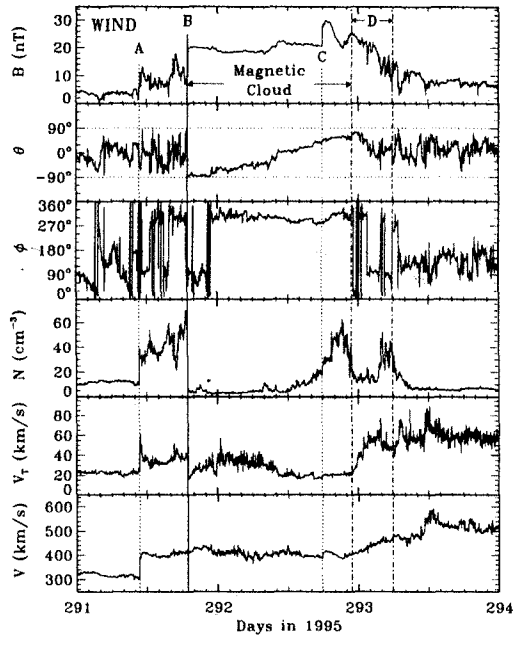

Figure 11. An unusual case of a compressive wave (c) within an interplanetary magnetic cloud.

A more probable mechanism will be shock compression of sheath plasmas. The August 1972 event was an event of this type. This is shown as Figure 12, adapted from Smith et al. (1976). Note that at Pioneer 10 distances (2.2 AU), there are 2 forward shocks and one reverse shock. The two fast forward shocks are presumably due to two fast CME injection events occurring at the Sun. The first forward shock compresses the ambient magnetic field from ~2 nT to ~8 nT and the second increases the field further from ~8 nT to ~16 nT. These are the highest magnetic field strengths of this compound interplanetary event, higher than the cloud field (the magnetic cloud is present from 12 UT day 220 to 16 UT day 221). The field within the magnetic cloud is primarily northwardly directed. The result from the interaction of the cloud with the Earth's magnetosphere was geomagnetic quiet (not shown).

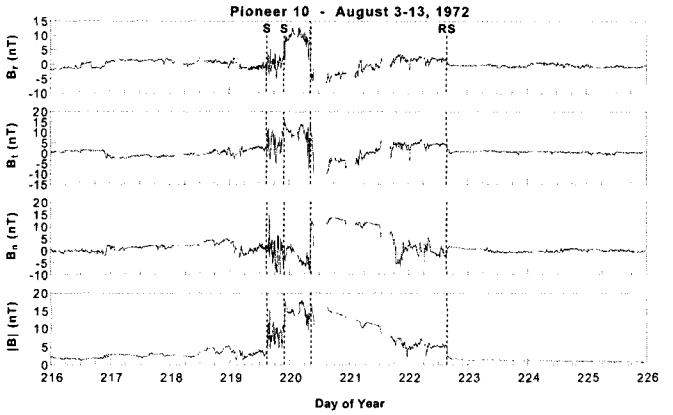

Figure 12. A shock within an interplanetary sheath event (double forward shocks). (taken from Tsurutani et al., 1992).

4.1.3 Multiple Magnetic Storms

Storms which occur in quick succession can increase the total ring current energy to give the appearance of a particularly large storm. Figure 13 shows the results of a superposed epoch analyses by Yokoyama and Kamide (1997) and Kamide et al. (1998b), for an examination of single storms and double storms. The top panel gives the AL index for single and double storm events. On the bottom are the IMF B_S events corresponding to the top panel events. For the double storm events where the second storms are more intense (of the two), the IMF B_S is approximately equal for the two events, indicating that there is some form of nonlinearity within the system. One possible explanation is that the plasmasheet becomes "primed" by hot oxygen ions (Kozyra et al., 2000) during the first storm, leading to a much more intense second event even though the interplanetary driver is essentially the same as for the first event. The interplanetary drivers of the two storms of double storms are: a) southward B_Z associated with the sheath and b) the magnetic cloud of the fast ICME (for the second storm). Thus if the sheath and the magnetic cloud fields associated with a fast ICME are both directed southward, the composite, "double storm" will be more intense than one might expect from the IMF B_S values.

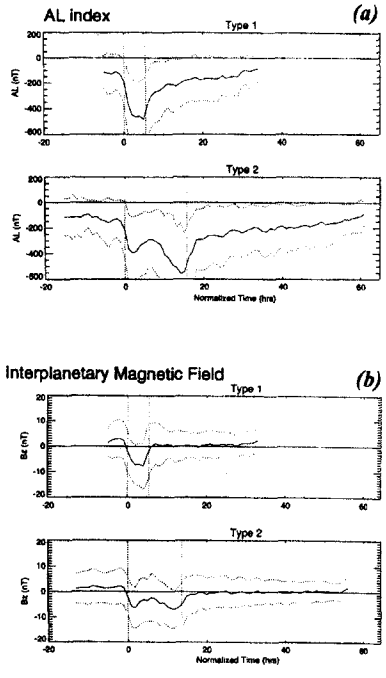

Figure 13. Superposed epoch analyses of single storms and "double" storm events. The interplanetary B_z components are given in Panel (b).

4.2 Geomagnetic Quiet

Intense, northward interplanetary magnetic fields like the August 1972 event lead to extreme geomagnetic quiet. For magnetic cloud cases where there are equal north and south IMF B_Z portions, the southward B_Z parts cause storm main phases and the northward B_Z parts cause geomagnetic quiet.

Table 1 gives the "efficiency" of solar wind coupling for 11 events where $B_N > +10$ nT and $T > 3$ hrs (during a solar maximum time period). Most of these events were portions of magnetic clouds. It was found that the average coupling efficiency for these 11 events was ~3 x 10^{-3}, i.e., ~0.3% of the incident solar wind ram energy gets into the magnetosphere. This efficiency is approximately 30 times less than during magnetic reconnection (IMF B_S) events.

TABLE 1. U_T and energy transfer efficiency

Date	UT	dE_{mag}/dt (erg s^{-1})	η efficiency

18 Dec 1978	0100	5.3×10^{17}	4.0×10^{-3}
21 Feb 1979	1200	2.2×10^{17}	1.0×10^{-3}
3 Apr 1979	1230	2.2×10^{17}	2.2×10^{-3}
5 Apr 1979	0300	6.0×10^{17}	3.0×10^{-3}
5 Apr 1979	1230	9.0×10^{17}	2.0×10^{-3}
29-30 May 1979	2130	4.5×10^{17}	7.1×10^{-3}
20 Aug 1979	0830	4.5×10^{17}	3.4×10^{-3}
18-19 Sep 1979	2400	1.1×10^{17}	1.3×10^{-3}
6 Oct 1979	1800	3.3×10^{17}	1.7×10^{-3}
7 Oct 1979	0800	1.1×10^{18}	1.1×10^{-3}
11 Nov 1979	1800	3.0×10^{17}	2.1×10^{-3}

5. DECLINING PHASE OF THE SOLAR CYCLE

5.1 Corotating Streams - CIRs

During the declining phase of the solar cycle, corotating high-speed streams emanating from coronal holes dominate geomagnetic activity. During this phase of the solar cycle, polar coronal holes expand in spatial extent and have portions that migrate toward and sometimes cross the ecliptic plane. These latter cases lead to solar wind streams which engulf the Earth's magnetosphere once per ~27 days. The streams thus cause ~27 day recurrence of small geomagnetic storms and recurrences of High Intensity Long Duration Continuous AE Activity (HILDCAA) events (Tsurutani and Gonzalez, 1987).

When the high-speed solar wind catches up with the slower speed solar wind, the interaction leads to a compression in plasma and magnetic fields. These compression regions are called Corotating Interaction Regions or CIRs.

Figure 14 shows a high-speed solar wind/slow speed solar wind interaction on January 24-27, 1974. The high-speed solar wind proper is to the right of the vertical dashed line, the undisturbed slow solar wind is on the far left of the figure. The interaction region is in the middle. The intense magnetic field region (shaded in the next to the bottom panel) is the CIR. The resultant small magnetic storm is shown in the bottom panel (D_{ST}).

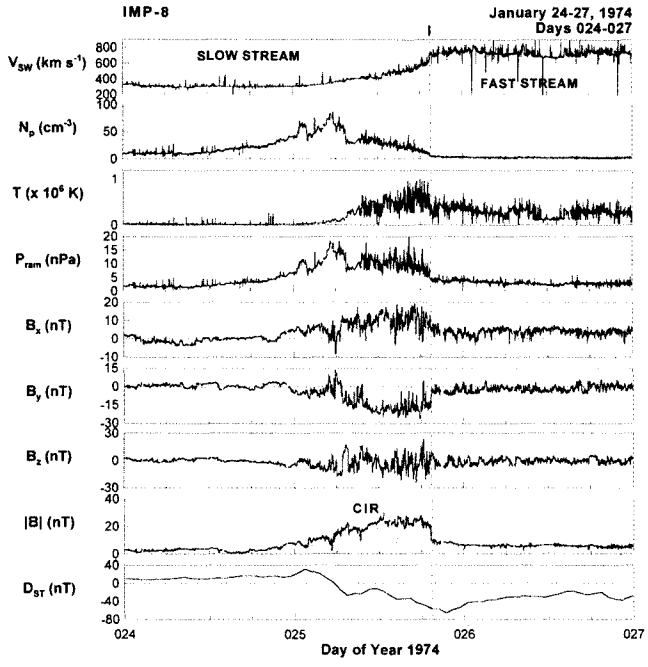

Figure 14. An example of a CIR. The high-speed stream (on the right) is colliding with a low-velocity high density heliospheric current sheet (HCS) plasmasheet, forming a compressed magnetic field region.

At distances of 1 AU from the Sun, CIRs typically do not have fast forward shocks (Tsurutani et al., 1995). Therefore there is no SSC associated with the storm initial phase for these events. The storm main phases are small and irregular in profile (in comparison to solar maximum/magnetic cloud related events shown earlier). The causes of the irregularly shaped D_{ST} indices are noted in the B_Z data. The B_Z component is highly fluctuating. The lack of a long, continuous southward B_Z leads to the small intensity of the magnetic storm, even though the B_S magnitudes are sometimes quite high.

5.2 HILDCAAs

The recovery phase of the storm in Figure 14 is quite long. The peak D_{ST} value of ~ -65 nT occurs at ~21:30 UT on day 25. The D_{ST} value is still depressed by the end of day 26.

The D_{ST} indices for all of 1974 are shown in Figure 15. There are only 3 large storm events with $D_{ST} < -100$ nT. Each of these have been shown to be

caused by ICMEs and/or their upstream sheaths (Tsurutani et al., 1995). The many smaller (recurrent) storms during 1974 are associated with CIRs interactions with the magnetosphere. However, what is particularly noteworthy in the figure are the intense AE events in each of the long storm "recovery phases". The recovery phases can last weeks or longer. The D_{ST} recoveries are associated with the high AE values. The average AE value for 1974 was 283 nT, whereas it was only 225 nT for 1979 (solar maximum)! *Thus averaging over a year, corotating streams can be more geoeffective in transferring solar wind energy into the magnetosphere than ICMEs during solar maximum.* This is because the substorms associated with the high-speed streams are occurring continuously (during the solar cycle declining phase), whereas magnetic storms are sporadic during solar maximum.

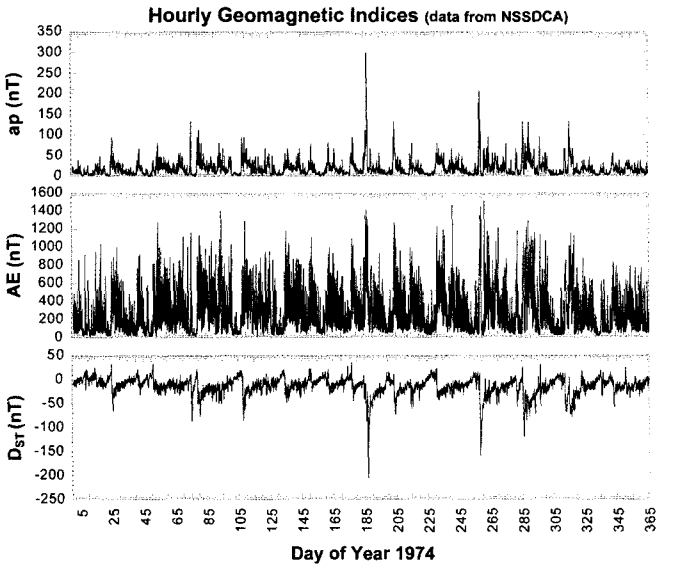

Figure 15. Ap, AE and D_{ST} for 1974. HILDCAAs are the high-intensity AE intervals following the small 27 day recurring magnetic storms. HILDCAAs are near-continuous substorms created by the Alfvén wave B_S fluctuations.

What is the interplanetary cause of these long duration storm recovery phases and high AE values? The answer is given in Figure 16. The interplanetary B_Z is highly fluctuating in this high velocity stream event. With every southward field turning, there is an increase in AE and decrease in D_{ST}. The southward field turnings cause magnetic reconnection and plasma injections into the nightside magnetosphere. There are slight D_{ST} decreases at each of these injections. These periods of continuous substorm activity are called HILDCAAs, and the sporadic injection of plasma into the

magnetosphere is the reason why the ring current does not appear to "decay". What is actually happening is the HILDCAAs are related to sporadic, low-intensity particle injections into the outer portions of the ring-current, thus the lack of an overall "decay" (Tsurutani et al., 1995).

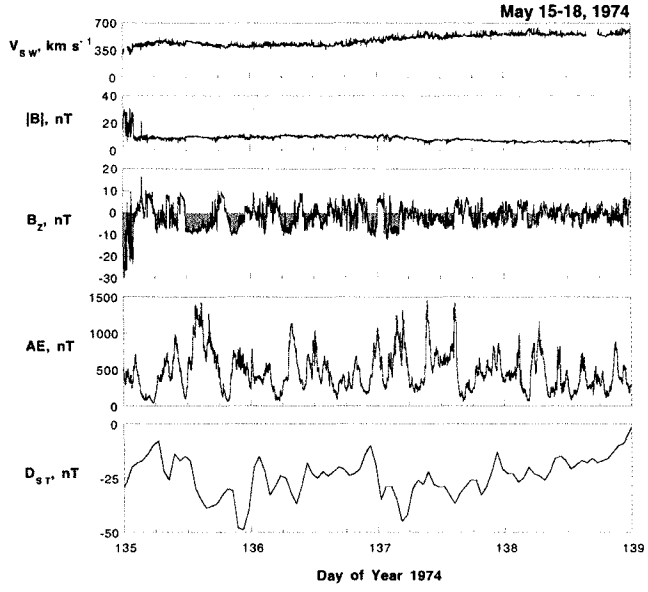

Figure 16. Interplanetary Alfvén waves, AE increases and D_{ST} decreases. The causes of long recovery phases in recurrent storms is due to sporadic magnetic reconnection (the IMF B_z component of the Alfvén waves), and consequential (substorm) injections of plasma into the magnetosphere.

The continuous presence of magnetospheric chorus plasma waves (and other wave modes) associated with HILDCAAs has been invoked (Horne and Thorne, 1998; Summers et al., 1998; 2000) to explain the magnetospheric relativistic electron events (Baker et al., 1989; Li et al., 1997) present in these intervals of high-speed solar wind streams. These relativistic electrons have been related to the possible failure of a Canadian telecommunication satellite.

What causes the interplanetary B_Z fluctuations? The NASA/ESA Ulysses mission has provided us with answers. Figure 17 shows the magnetic field and plasma components taken over the solar north pole within a high-speed solar wind stream (coming from a polar coronal hole). Continuous fluctuations are noted in all of the magnetic field and velocity components. When these fluctuations are analyzed (by performing cross-correlations between the B and V components), it is found that the

components are highly correlated at zero lag. Belcher and Davis (1971) have demonstrated that this indicates that these are Alfvén waves. The waves are determined to be propagating away from the Sun (determined by the sign of the correlation coefficient). Thus the Alfvén waves present in the high-speed streams lead to the B_Z fluctuations within the CIRs (the waves are compressed) leading to the irregularly shaped storm main phase, and also are the fluctuations that cause HILDCAAs in the storm "recovery phases".

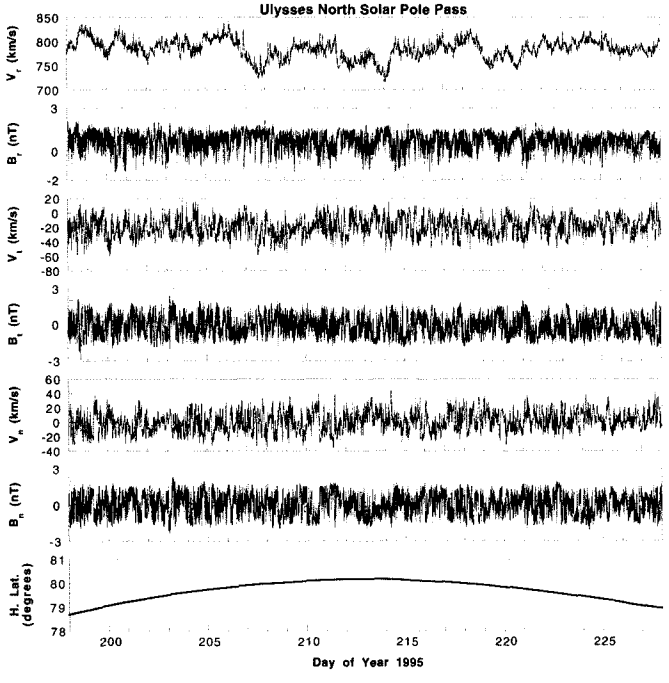

Figure 17. Alfvén waves measured in a high-speed stream (of coronal hole origin).

For visualization purposes, a two-dimensional schematic of the high-speed/slow-speed solar wind stream interactions is shown in Figure 18. Note the interface (IF) between the slow-speed stream and high-speed stream is a tangential discontinuity. The Alfvén waves of the high-speed stream are amplified by compression at the reverse shock (RS).

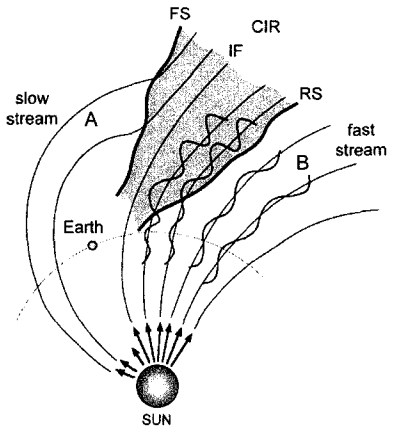

Figure 18. A schematic of a high-speed/slow-speed stream interaction and CIR formation.

In summary, a profile of magnetic storms during the declining phase of the solar cycle is given in Figure 19. The initial phase does not start suddenly (there is no SSC). The main phase is small and irregularly shaped, and the recovery phase is irregularly shaped and of long duration.

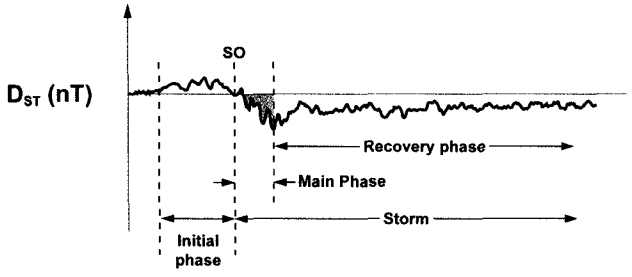

Figure 19. An idealised profile of a magnetic storm in the declining phase of the solar cycle.

5.3 Geomagnetic Quiet

What causes geomagnetic quiet during the declining phase of the solar cycle? Figure 15 can be used to identify such regions. AE and Ap have particularly low values at the trailing ends of the streams and are located at times occurring after the HILDCAA events. D_{ST} is generally positive, indicative of high plasma density regions (increased ram pressure). Figure 20 shows the solar wind plasma, magnetic field and D_{ST} indices for the entire year 1974. Using the positive D_{ST} events as markers, we find that the geomagnetically quiet intervals occur at the ends of the high-speed streams and at the beginnings of the heliospheric current sheet plasma sheet regions

(see sector boundary markers at top). The ends of high speed streams are characterized by low plasma velocities, low plasma densities, low magnetic field magnitudes and the absence of B_Z fluctuations. The second region, the heliospheric current sheet plasmasheet, is characterized by high plasma densities. Both of these regions contribute to geomagnetic quiet during the declining phase of the solar cycle. The cause of the geomagnetically quiet intervals is the lack of magnetic reconnection between the interplanetary medium and the magnetosphere.

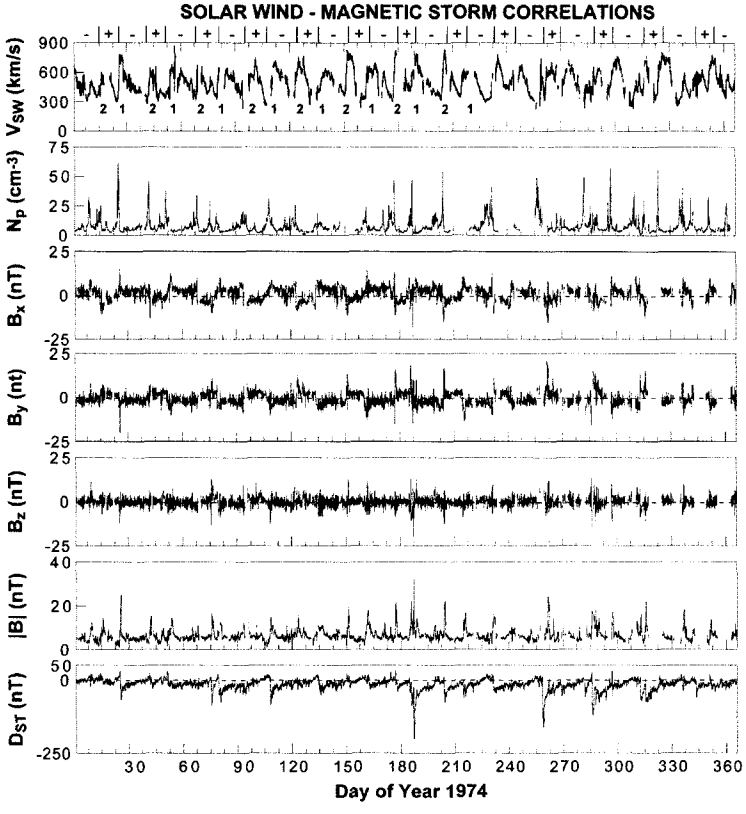

Figure 20. The solar wind plasma, magnetic field, and D_{ST} indices for year 1974.

6. SHOCK-AURORAS AT EARTH, JUPITER AND SATURN

It has recently been shown that the shocks found ahead of fast ICMEs cause energy transfer directly into the (dayside) magnetosphere, rather than

by transport first to the magnetotail and then to the nightside magnetosphere in the case of magnetic reconnection discussed earlier. When the ram pressure pulses (associated with interplanetary shocks) compress the Earth's magnetosphere, dayside auroras result almost instantaneously. Figure 21 is an example of a shock-aurora event taken by Polar UVI imaging instrument. The images are the LBH long wavelength images displayed in magnetic local time (MLT) coordinates. The north pole is at the center, and 60° latitude local noon is at the top in each panel. Dawn is to the right and dusk to the left. The time sequence goes from the top left to the right. Each image is separated by ~3 min 4 s. The January 10, 1997 event is shown. Using the solar wind speed measured by WIND and the shock speed calculated from the Rankine-Hugoniot conservation equations, the shock arrival time at the magnetopause was calculated. The arrival time was determined to occur between the second and third images of the figure. At the third image, 01:03:48 UT, there is a brightening of the aurora on the dayside from 10 to 12 MLT at ~75° latitude. This brightening is within the auroral oval. With time, the brightening spreads towards both dawn and dusk until the whole oval (less the midnight sector) is intensified (by 0113:00 UT).

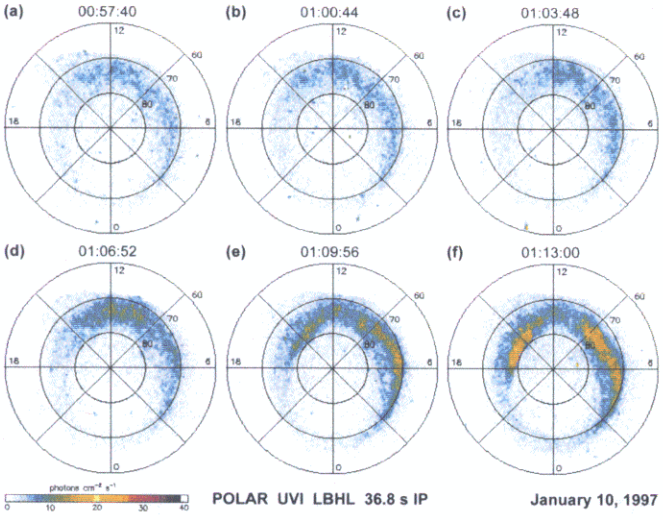

Figure 21. A dayside aurora caused by an interplanetary shock (a shock-aurora). (taken from Zhou and Tsurutani, 1999)

Nine interplanetary shock events were detected in 1997 when Polar had clear viewing of the dayside auroral zone. For these cases, "dayside" auroras occurred each time. The velocities of the aurora in the ionosphere are shown in Table 2, Column 2. Three events are listed. The velocities

range from 6 to 11 km s^{-1}, much higher than the standard <1 km s^{-1} detected for substorm or storm nightside auroras. If the ionospheric velocities are extrapolated to the equatorial plane of the same magnetic field lines, the velocities (at the magnetopause) will be 280 to 370 km s^{-1}. These speeds are quite similar to that of the measured solar wind speeds for these events (see Column 4). Thus the speed of the aurora as it propagates from noon to dawn and dusk is associated with the antisunward propagation of the shock pressure pulse along the magnetopause boundary.

TABLE 2. Ionospheric auroral "speed", mapped into the magnetosphere, and solar wind velocity

Event	Ionospheric V (km/s)	Mapped V* (km/s)	Observed $V_{sh/sw}$ (km/s)	Spacecraft Position (R_e)
10 Jan 1997	6 (dusk)	280	300	I-T (Sheath) (-19, 19, 10)
1 Oct 1997	10 (dusk)	370	460	IMP-8 (SW) (10, 32, -3)
10 Dec 1997	11 (dawn)	365	360	GT (SW) (-4, -25, -0.5)

* Assuming a dipole field of L=10

Shock created auroras are fainter than those of substorm auroras, but because of the much greater latitudinal extent of the former, the energy deposition rate is ~5 times greater than that of a moderate substorm (Tsurutani et al., 2001a).

The specific mechanisms for solar wind energy transfer into the magnetosphere are uncertain at this time. Two possibilities have been suggested in the literature and are schematically illustrated in Figure 22a and b. In Figure 22a, the interplanetary shock compresses outer zone magnetospheric magnetic fields and preexisting plasma. The heating of the plasma in the direction perpendicular to the field leads to temperature anisotropies and the loss cone instability. The loss of these energetic charged particles to the ionosphere would result in a diffuse aurora. A second mechanism (Figure 22b) is that shock compression of the outer zone dayside magnetosphere creates field-aligned potentials that accelerate electrons into the ionosphere. The precipitating electrons will create auroral arcs.

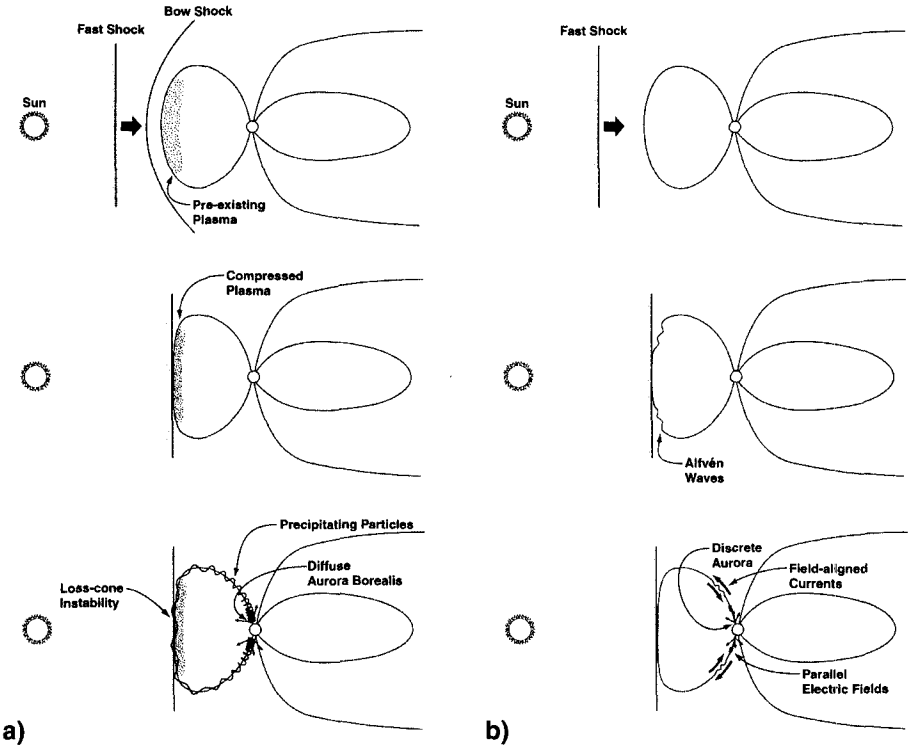

Figure 22. Two possible mechanisms for shock-aurora formation.

To determine whether one, both, or none of these mechanisms are correct, it would be extremely useful to have ground based observations to determine what types of auroral forms are created by interplanetary shock compression. Unfortunately, ground-based observations have not been reported for these types of events to date.

Perhaps our first test of these models might occur with auroral observations at Jupiter. Jovian UV auroras have been detected from observations made using the Hubble Space Telescope (HST) (Prangé et al., 1993; Clarke et al., 1998). An example of a Jovian polar aurora is shown in Figure 23. Note that there are two auroral rings. The brightest one occurs at $L \approx 20\text{-}30$ (Prangé et al., 1997) and a fainter one poleward of this. This latter feature could correspond to the magnetopause boundary layer, similar to the situation at Earth.

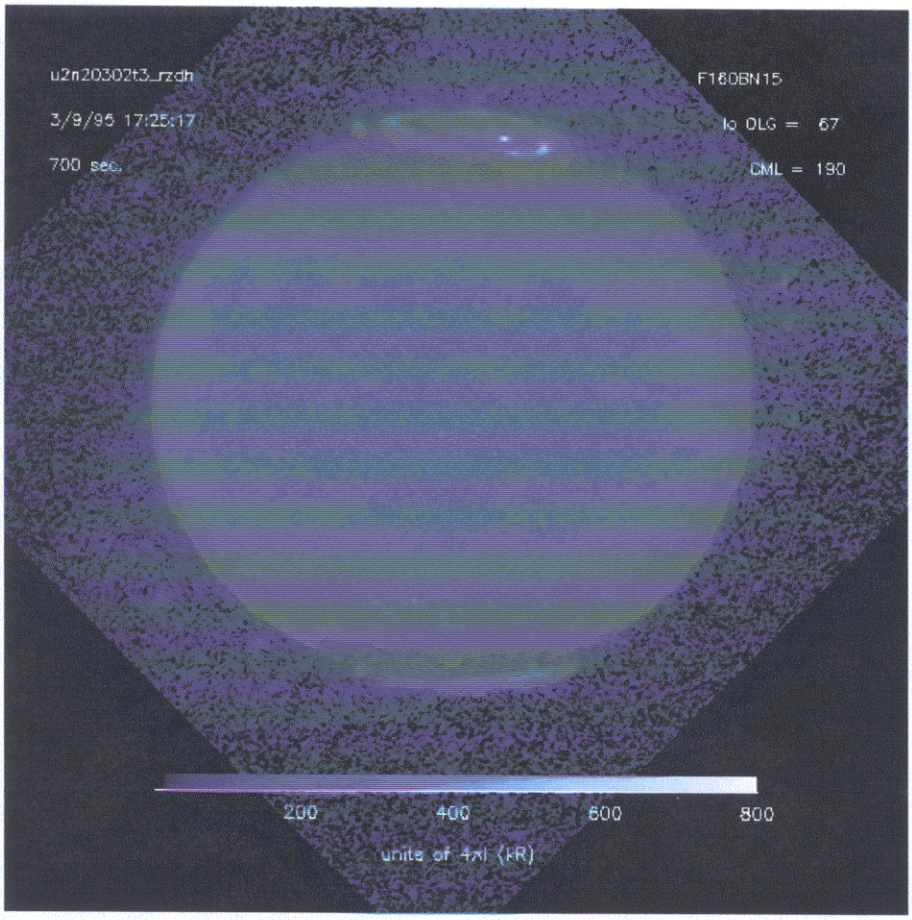

Figure 23. Jovian UV aurora. There are two auroral rings, in this instance.

Following Haerendel (1994), the potential drops along the Jovian magnetic fields have been calculated (Tsurutani et al., 2001b). Input values used for the calculation were a magnetopause field strength of 5 nT, plasma density of 0.1 cm^{-3}, a measured magnetopause/boundary layer width of ~7000 km (Sonnerup et al., 1981), and a shock "perturbation" field of 5 nT. Using the above numbers, a parallel potential drop of ~50 kV was determined. It happens that ~50 keV electrons are needed to explain the Jovian aurora spectroscopic measurements (H. Waite, private communication, 2000), so this mechanism may indeed explain the higher latitude auroral ring.

In the near future, Cassini will fly past Jupiter, measuring the interplanetary medium and imaging the aurora. Galileo will be inside the

magnetosphere determining the state of the radiation belts and imaging instruments will also be observing the aurora. HST will be viewing Jupiter's UV aurora as the Cassini flyby takes place. Jovian polar auroras sometimes episodically reach intensities of more than a megarayleigh (10^{12} photons cm^{-2} s^{-1}), 10 to 100 times more intense than that for the Earth's auroras (J. Clarke, personal communication, 2000). It will be interesting to see if these particularly intense auroras are caused by interplanetary shocks and if so, if they are discrete or diffuse auroras.

ACKNOWLEDGEMENT

Portions of the research reported here were performed at the Jet Propulsion Laboratory, California Institute of Technology, Pasadena, California under contract with the National Aeronautics and Space Administration, Washington DC. The author wishes to thank W.D. Gonzalez and K. Papadopoulos for critical readings of the manuscript.

REFERENCES

Alfvén, H., and C.-G. Fälthammer, *Cosmic Electrodynamics*, Oxford, 1967.

Araki, T., Global structure of geomagnetic sudden commencements, *Planet. Space Sci.*, **25**, 373, 1977.

Araki, T., A physical model of geomagnetic sudden commencement, in *Solar Wind Sources of Magnetospheric Ultra Low Frequency Waves*, edited by M. Engebretson, K. Takahashi, and M. Scholer, 81, 183, Amer. Geophys. Un. Press, Washington D.C., 1994.

Baker, D.N., et al., Relativistic electrons near geostationary orbit: Evidence for internal magnetospheric acceleration, *Geophys. Res. Lett.*, **16**, 559, 1989.

Belcher, J.W., and L. Davis Jr., Large amplitude Alfvén waves in the interplanetary medium, 2, *J. Geophys. Res.*, **76**, 3534, 1971.

Campbell, W.H., Comment on "Current understanding of magnetic storms: Storm-substorm relationships" by Y. Kamide et al., *J. Geophys. Res.*, **104**, 7049, 1999.

Chapman, S., and J. Bartels, *Geomagnetism, 1*, Clarendon, Oxford, 1940.

Clarke, J.T., G. Ballester, J. Trauger, J. Ajello, W. Prior, K. Tobiska, J.E.P. Connerney, G.R. Gladstone, J.H. Waite, L.B. Jaffel, and J.-C. Gerard, Hubble Space Telescope imaging of Jupiter's UV aurora during the Galileo orbiter mission, *J. Geophys. Res.*, **103**, 20217, 1998.

Dessler, A.J., and E.N. Parker, Hydromagnetic theory of magnetic storms, *J. Geophys. Res.*, **64**, 2239, 1959.

Dungey, J.W., Interplanetary magnetic field and the auroral zones, *Phys. Res. Lett.*, **6**, 47, 1961.

Farrugia, C.J., L.F. Burlaga, and R.P. Lepping, Magnetic clouds and the quiet storm effect at Earth, in *Magnetic Storms*, edited by B.T. Tsurutani, W.D. Gonzalez, Y. Kamide and J.K. Arballo, AGU Press, Wash. D.C., **98**, 91, 1997.

Fox, N.J., M. Paredo, and B.J. Thompson, Cradle to grave tracking of the January 6-11, 1997 Sun-Earth Connection Event, *Geophys. Res. Lett.*, **25**, 2461, 1998.

Gonzalez, W.D., and F.S. Mozer, A quantitative model for the potential resulting from reconnection with an arbitrary interplanetary magnetic field, *J. Geophys. Res.*, **79**, 4186, 1974.

Gonzalez, W.D., and B.T. Tsurutani, Criteria of interplanetary parameters causing intense magnetic storms (D_{ST} < -100 nT), *Planet Space Sci.*, **35**, 1101, 1987.

Gonzalez, W.D., J.A. Joselyn, Y. Kamide, H.W. Kroehl, G. Rostoker, B.T. Tsurutani, and V.M. Vasyliunas, What is a geomagnetic storm?, *J. Geophys. Res.*, **99**, 5771, 1994.

Haerendel, G., Acceleration from field-aligned potential drops, *Astrophys. J. Suppl.*, **90**, 765, 1994.

Horne, R.B., and R.M. Thorne, Potential waves for relativistic electron scattering and stochastic acceleration during magnetic storms, *Geophys. Res. Lett.*, **25**, 3011, 1998.

Kamide, Y., W. Baumjohann, I.A. Daglis, W.D. Gonzalez, M. Grande, J.A. Joselyn, R.L. McPherron, J.L. Phillips, E.G.D. Reeves, A.S. Sharma, H.J. Singer, B.T. Tsurutani, and V.M. Vasyliunas, Current understanding of magnetic storms: Storm-substorm relationships, *J. Geophys. Res.*, **103**, 17705, 1998a.

Kamide, Y., N. Yokoyama, W. Gonzalez, B.T. Tsurutani, I.A. Daglis, A. Brekke, and S. Masuda, Two-step development of geomagnetic storms, *J. Geophys. Res.*, **103**, 6917, 1998b.

Kamide, Y., W. Baumjohann, I.A. Daglis, W.D. Gonzalez, M. Grande, J.A. Joselyn, R.L. McPherron, J.L. Phillips, E.G.D. Reeves, G. Rostoker, A.S. Sharma, H.J. Singer, B.T. Tsurutani, and V.M. Vasyliunas, Reply, *J. Geophys. Res.*, **104**, 7051, 1999.

Kennel, C.F., J.P. Edmiston, and T. Hada, A quarter century of collisionless shock research, in *Collisionless Shocks in the Heliosphere: A Tutorial Review*, AGU Press, Wash. D.C., **34**, 1, 1985.

Kennel, C.F., and H.E. Petschek, Limit on stably trapped particle fluxes, *J. Geophys. Res.*, **71**, 1, 1996.

Klein, L.W., and L.F. Burlaga, Interplanetary magnetic clouds at 1 AU, *J. Geophys. Res.*, **87**, 613, 1982.

Kozyra, J.U., V.K. Jordanova, R.B. Horne, and R.M. Thorne, Modeling of the contribution of electromagnetic ion cyclotron (EMIC) waves to stormtime ring-current erosion, in *Magnetic Storms*, edited by B.T. Tsurutani, W.D. Gonzalez, Y. Kamide, and J.K. Arballo, AGU Press, Wash. D.C., **98**, 187, 1997.

Lepping, R.P., L.F. Burlaga, A. Szabo, K.W. Ogilvie, W.H. Mish, D. Vassiliadis, A.J. Lazarus, J.T. Steinberg, C.J. Farrugia, L. Janoo, and F. Mariani, The wind magnetic cloud and events of Oct. 18-20, 1998: Interplanetary properties and triggering for geomagnetic activity, *J. Geophys. Res.*, **102**, 14049, 1997.

Li, X., et al., Multisatellite observations of the outer zone electron variation during the November 3-4, 1993 magnetic storm, *J. Geophys. Res.*, **102**, 14123, 1997.

Northrup, T.G., The guiding center approximate to charged particle motion, *Ann. Phys.*, **15**, 79, 1961.

Prangé, R., M. Dougherty, and V. Dols, Identification d'une aurorae, "current-driven" sur Jupiter, á l'aide d'observations corréleés avec HST et Ulysses, in *Compte-redus du Séminaire scientifique du GdR Plasmae*, ed. D. Hubert, DESPA - Observatoire du Paris, 38, 1993.

Prangé, R., S. Maurice, W.M. Harris, D. Rego, and T. Livengood, Comparison of IUE and HST diagnostics of the Jovian Aurorae, *J. Geophys. Res.*, **102**, 9289, 1997.

Sckopke, N., A general relation between the energy of trapped particles and the disturbance field near the Earth, *J. Geophys. Res.*, **71**, 3125, 1966.

Smith, E.J., The August 1972 solar terrestrial events: Interplanetary magnetic field observations, *Space Sci. Rev.*, **19**, 661, 1976.

Summers, D., R.M. Thorne, and F. Xiao, Relativistic theory of wave-particle resonant diffusion with application to electron acceleration in the magnetosphere, *J. Geophys Res.*, **103**, 20487, 1998.

Summers, D., and C.-Y. Ma, A model for generating relativistic electrons in the Earth's inner magnetosphere based on gyroresonant wave-particle interactions, *J. Geophys. Res.*, **105**, 2625, 2000.

Tsurutani, B.T., and R.P. Lin, Acceleration of >47 keV ions and >2 keV electrons by interplanetary shocks at 1 AU, *J. Geophys. Res.*, **90**, 1, 1985.

Tsurutani, B.T., and W.D. Gonzalez, The cause of high intensity long-duration continuous AE activity (HILDCAAs): Interplanetary Alfvén wave trains, *Planet. Space Sci.*, **35**, 405, 1987.

Tsurutani, B.T., B.E. Goldstein, W.D. Gonzalez, and F. Tang, Comment on "A new method of forecasting geomagnetic activity and proton showers", by A. Hewish and P.J. Duffet-Smith, *Planet. Space Sci.*, **36**, 205, 1988a.

Tsurutani, B.T., W.D. Gonzalez, F. Tang, S.-I. Akasofu, and E.J. Smith, Origin of interplanetary southward magnetic storms near solar maximum (1978-1979), *J. Geophys. Res.*, **93**, 8519, 1988b.

Tsurutani, B.T., W.D. Gonzalez, F. Tang, and Y.T. Lee, Great magnetic storms, *Geophys. Res. Lett.*, **19**, 73, 1992.

Tsurutani, B.T., W.D. Gonzalez, F. Tang, Y.T. Lee, M. Okada, and D. Park, Reply to L.J. Lanzerotti, *Geophys. Res. Lett.*, **19**, 1993, 1992.

Tsurutani, B.T., W.D. Gonzalez, A.L.C. Gonzalez, F. Tang, J.K. Arballo, and M. Okada, Interplanetary origin of geomagnetic activity in the declining phase of the solar cycle, *J. Geophys. Res.*, **100**, 21717, 1995.

Tsurutani, B.T., and W. D. Gonzalez, The efficiency of "viscous interaction" between the solar wind and the magnetosphere during intense northward IMF events, *Geophys. Res. Lett.*, **22**, 663, 1995.

Tsurutani, B.T., and W.D. Gonzalez, The interplanetary causes of magnetic storms: A review, in *Magnetic Storms*, edited by B.T. Tsurutani, W.D. Gonzalez, Y. Kamide and J.K. Arballo, AGU Press, Wash. D.C., **98**, 77, 1997.

Tsurutani, B.T., and G.S. Lakhina, Some basic concepts of wave-particle interactions in collisionless plasmas, *Rev. Geophys.*, **35**, 491, 1997.

Tsurutani, B.T., Y. Kamide, J.K. Arballo, W.D. Gonzalez, and R.P. Lepping, Interplanetary causes of great and superintense magnetic storms, *Phys. Chemistry Earth*, **24**, 101, 1999.

Tsurutani, B.T., X.-Y. Zhou, J.K. Arballo, W.D. Gonzalez, G.S. Lakhina, V. Vasyliunas, J.S. Pickett, T. Araki, H. Yang, G. Rostoker, T.J. Hughes, R.P. Lepping, and D. Berdichevsky, Auroral zone dayside precipitation during magnetic storm initial phases, *J. Atmosph. Solar Terr. Phys.*, in press, 2001a.

Tsurutani, B.T., X.-Y. Zhou, V.M. Vasyliunas, G. Haerendel, and J.K. Arballo, Interplanetary shocks, magnetopause boundary layers and dayside auroras, to appear in *Surveys in Geophys.*, 2001b.

Von Humboldt, A., Magnetische Ungewitter, *Annales der Physik*, **29**, 25, 1808.

Yokoyama, N., and Y. Kamide, Statistical nature of geomagnetic storms, *J. Geophys. Res.*, **102**, 14215, 1997.

Zhou, X.-Y., and B.T. Tsurutani, Rapid intensification and propagation of the dayside aurora: Large scale interplanetary pressure pulses (fast shocks), *Geophys. Res. Lett.*, **26**, 1097, 1999.